*Journal of the European Ceramic Society* **14** (1994) 13–21

# Preparation and Grain Boundary Devitrification of Samarium α-Sialon Ceramics

Yi-Bing Cheng

Department of Materials Engineering, Monash University, Australia

&

Derek P. Thompson

Department of Mechanical, Materials & Manufacturing Engineering, University of Newcastle upon Tyne, UK

(Received 26 October 1993; accepted 20 December 1993)

## *Abstract*

*The reaction sequence and densification behaviour of Sm α-sialon ceramics have been studied.* $Sm_2O_3$ *is an effective sintering aid and dense Sm α-sialon ceramics can be prepared by pressureless sintering at 1800°C for 4 h. Post-sintering heat-treatment produces two different grain boundary phases depending on the heat-treatment temperature. Below 1400°C* $SmAlO_3$ *is stable, and between 1400 and 1600°C an Al-containing melilite solid solution* ($M'_{SS}$) *appears at the grain boundaries. Microstructures of the materials before and after heat-treatment have been studied and the results are discussed.*

*Die Reaktionssequenz und das Verdichtungsverhalten von Sm α-Sialonkeramiken wurde untersucht.* $Sm_2O_3$ *ist eine effektive Sinterhilfe, die es erlaubt, Sm α-Sialonkeramiken durch druckloses Sintern bei 1800°C und einer Sinterzeit von 4 Stunden herzustellen. Wärmebehandlungen nach dem Sintern ergeben zwei verschiedene Korngrenzenphasen, die von der Wärmebehandlungstemperatur abhängen.* $SmAlO_3$ *ist unterhalb von 1400°C stabil. Zwischen 1400 und 1600°C entsteht an den Korngrenzen ein Melititmischkristall* ($M'_{SS}$)*, der Al enthält. Die Gefüge wurden vor und nach der Wärmebehandlung untersucht. Die Ergebnisse werden im folgenden diskutiert.*

*La séquence des réactions et le comportement à la densification de céramiques en α-sialon contenant Sm ont été étudiés.* $Sm_2O_3$ *est un additif de frittage efficace et des céramiques Sm α-sialon denses peuvent être préparées par frittage naturel à 1800°C durant 4 h. Un traitement thermique après frittage produit deux phases différentes aux joints de grains, selon la température de traitement. Sous 1400°C,* $SmAlO_3$ *est stable et entre 1400 et 1600°C, une solution solide de type melilite, contenant Al*($M'_{SS}$) *se forme aux joints de grains. Les microstructures des matériaux avant et après traitement thermique on été étudiées et les résultats sont discutés.*

## 1 Introduction

It is essential to add densifying additives for successful pressureless sintering of silicon nitride materials because of the strong covalent characteristic of the silicon–nitrogen bond which results in insufficient diffusion at sintering temperatures. With increase in temperature, the added oxides react with the silica on the surface of the silicon nitride powder, giving an oxynitride liquid which helps the transformation from α-silicon nitride to the β form and assists densification. However, vitreous or secondary crystalline phases are produced after cooling, which impair high-temperature mechanical properties, such as strength and creep resistance.

α-Sialon (α′), unlike β-sialon (β′), can accommodate additional cations into its structure. It offers at least two promising advantages over β′, namely, increased hardness and the possibility of producing a single-phase ceramic with a minimum of grain boundary phases. A successful oxide additive ($RO_x$) for α′ ceramics should satisfy the following criteria: (1) the cation R must be able to stabilise the α′ structure; (2) the eutectic temperature of the oxide-containing liquid should be lower than the formation temperature of the α′

phase but high enough to give good creep behaviour, (3) no intermediate phase produced by the oxide during sintering should prevent densification and remain in the final product; (4) it is desirable but not essential to have a large liquid-phase region in the R–Si–Al–O–N system in equilibrium with the $\alpha'$ phase; (5) the crystalline phases devitrified from the R-containing grain boundary glass should be oxidation and high-temperature resistant. The general formula for $\alpha'$ can be expressed as $R_xSi_{12-(m+n)}Al_{m+n}O_nN_{16-n}$, where R is a large cation (typically Li, Mg, Ca, Y and Ln with $Z \geq 60$) and $0 < x \leq 2$. Although a number of cations can stabilise $\alpha'$ structures, extensive studies have mainly been carried out in the yttrium-containing system.[1] Because of the high nitrogen content, densification of $\alpha'$ materials by pressureless sintering has been the major concern. Previous work has indicated the difficulties of achieving good densification and phase purity especially for rare earth $\alpha'$ ceramics.[2–4] It has been found that very few oxides can satisfactorily meet all the above demands and this has restricted the development of $\alpha'$ ceramics. Commercially $\alpha'$ phases have only found their place in the advanced ceramics market place as a second phase in $\alpha'$–$\beta'$ ceramic composites, where the better strength and easier densification of the $\beta'$ phase supplement the higher hardness of $\alpha'$.

In this paper, the role of samarium oxide in the densification of $\alpha'$ materials and subsequent devitrification of grain boundary glass has been examined and some comparisons are made between Sm-containing materials and other sialon systems.

## 2 Experimental

Based on previous studies[5] two basic compositions were selected (Table 1). $Si_3N_4$ (Starck, Berlin, LC10), AlN (Starck, Berlin, Grade B), $Al_2O_3$ (Alcoa, A17) and $Sm_2O_3$ (RE Acton, Rare Earth Products, 99·9%) powders were used as the starting materials in the preparation of $\alpha'$ samples. About 50 grams of powder and 150 $cm^3$ of isopropanol were mixed in a rubber-lined mill with 300 grams of $Si_3N_4$ balls for 3 days. Pellets of dried powders (about 6–10 grams) were first pressed in a steel die, followed by isostatic pressing under a pressure of 160 MPa. This usually produces a green body with approximately 60% theoretical density. Sintering was carried out in a carbon resistance furnace at different temperatures in a nitrogen atmosphere. All samples were placed in a carbon crucible embedded in a mixture of $Si_3N_4$ and BN packing powders. From room temperature to 1850°C, the heating rate of the furnace was 45°C/min and the natural cooling rate was about 50°C/min from 1850 to 1200°C. Heat-treatment was carried out in an alumina tube furnace in flowing nitrogen.

Crystalline phases were characterised using a Hägg–Guinier focusing camera with Si as a reference standard. The measurement of X-ray films and refinement of lattice parameters were carried out by a computer-linked SCANPI system (Arrhenius laboratory, University of Stockholm). A Camscan S4-80DV microscope with a windowless X-ray detector was used for SEM observation and EDAX analysis. Bulk densities of sintered samples were measured using water immersion. All specimens were boiled in water for one hour prior to density measurement.

## 3 Results and Discussion

### 3.1 Reaction sequence in the preparation of samarium $\alpha'$ ceramics

The two compositions were fired at temperatures between 1200 and 1850°C for 1 h respectively and cooled by switching off the furnace at the sintering temperature. These two samples were also hot-pressed at 1800°C under a pressure of 20 bar for 1 h, the purpose of which was to use the densities of the hot-pressed samples as reference standards against which to compare the pressureless sintered ones. X-Ray results and densities of samples after sintering are shown in Tables 2 and 3.

It can be seen from the tables that with increasing temperature, the first reaction to occur is that between $Sm_2O_3$ and $Al_2O_3$ at about 1200°C, leading to the formation of $SmAlO_3$. Above 1400°C $SmAlO_3$ started to react with $Si_3N_4$ and formed a liquid, from which a melilite solid solution phase, $M'_{SS}$, ($Sm_2Si_{3-x}Al_xO_{3+x}N_{4-x}$, $0 \leq x \leq 1$)[6] was precipitated. The formation of $M'_{SS}$ accelerated the dissolution of silicon nitride grains and resulted in an initial stage of densification. The amount of $M'_{SS}$ passed through a maximum between 1500 and 1600°C and then decreased as $M'_{SS}$ redissolved in the liquid with further increase in temperature. The transition from $\alpha$-$Si_3N_4$ to $\alpha'$ and $\beta'$ phases, through a transient liquid, took place above 1550°C and was complete at 1800°C with the complete disappearance of $M'_{SS}$.

The compositions of samples SA400 and SA800 are similar and show almost identical reaction sequences. At the end of the reaction, SA400 consisted mainly of $\alpha'$ and a trace of 21R, whereas SA800 contained $\alpha'$, 21R and a small amount of $\beta'$ as well. The 21R sialon polytypoid phase appeared at 1500°C and seemed to be in equilibrium with $\alpha'$ and $\alpha'$ + $\beta'$ phases, although 12H was

**Table 1.** The two principal Sm α' compositions used in this research

| | *$Si_3N_4$ (wt %)* | *AlN (wt %)* | *$Al_2O_3$ (wt %)* | *$Sm_2O_3$ (wt %)* | |
|---|---|---|---|---|---|
| SA400 | 67·62 | 19·09 | 2·00 | 11·29 | |
| SA800 | 72·50 | 14·27 | 2·00 | 11·23 | |
| | *$Si_3N_4$ (mol %)* | *AlN (mol %)* | *$Al_2O_3$ (mol %)* | *$Sm_2O_3$ (mol %)* | |
| SA400 | 48·22 | 46·58 | 1·96 | 3·24 | |
| SA800 | 56·37 | 37·97 | 2·14 | 3·52 | |
| | *$Si^{4+}$ (eq. %)* | *$Al^{3+}$ (eq. %)* | *$Sm^{3+}$ (eq. %)* | *$N^{3-}$ (eq. %)* | *$O^{2-}$ (eq. %)* |
| SA400 | 77·20 | 20·21 | 2·59 | 95·84 | 4·16 |
| SA800 | 82·06 | 15·38 | 2·56 | 95·88 | 4·12 |
| | *Actual formula*[a] | | | *k*[b] | |
| SA400 | $Sm_{0\cdot404}Si_{8\cdot919}Al_{3\cdot112}O_{1\cdot671}N_{14\cdot298}$ | | | 0·753 | |
| SA800 | $Sm_{0\cdot379}Si_{9\cdot548}Al_{2\cdot381}N_{1\cdot597}$ | | | 0·742 | |

[a] The actual compositions after correction for 1·98 and 2 wt % of oxygen on the surfaces of $Si_3N_4$ and AlN powders respectively.
[b] The atomic ratio $k = (Si + Al)/(O + N)$.

**Table 2.** Crystalline phases and densities of SA400 samples sintered at different sintering temperatures for 1 h

| *Sintering temperature (°C)* | *ΔW %* | *D ($gcm^{-3}$)* | *% of $D_{hp}$*[a] | *α* | *β* | *AlN* | *$Sm_2O_3$* | *$Al_2O_3$* | *α'* | *β'* | *$SmAlO_3$* | *$M'_{SS}$* | *21R* |
|---|---|---|---|---|---|---|---|---|---|---|---|---|---|
| Green body | — | 2·083 | 61 | vs | w | m | m | — | — | — | — | — | — |
| 1200 | 0 | 2·174 | 63 | vs | w | m | vvw | — | — | — | ms | — | — |
| 1300 | 0 | 2·171 | 63 | vs | w | m | — | — | — | — | ms | — | — |
| 1400 | 0·1 | 2·234 | 65 | vs | w | m | — | — | — | — | m | vw | — |
| 1500 | 1·0 | 2·356 | 69 | s | w | w | — | — | vw | — | — | m | vw |
| 1600 | 1·2 | 2·357 | 69 | m | w | w | — | — | m | — | — | m | vw |
| 1700 | 2·2 | 2·565 | 75 | vw | — | — | — | — | s | — | — | w | w |
| 1750 | 5·4 | 2·675 | 78 | — | — | — | — | — | vs | — | — | w | w |
| 1800 | — | 3·083 | 90 | — | — | — | — | — | vs | — | — | — | w |
| 1850 | 6·0 | 3·149 | 92 | — | — | — | — | — | vs | — | — | — | w |
| HP 1800 | 0·1 | 3·440 | 100 | — | — | — | — | — | vs | — | — | | w |

[a] Relative density compared with that of hot-pressed value.
α and β: α- and β-$Si_3N_4$; α' and β': α- and β-sialons; $M'_{SS}$: melilite solid solutions ($Sm_2Si_{3-x}Al_xO_{3+x}N_{4-x}$); 21R: sialon polytypoid.
X-Ray intensities: s, strong; m, medium; w, weak; v, very.

**Table 3.** Crystalline phases and densities of SA800 samples sintered at different sintering temperatures for 1 h

| *Sintering temperature (°C)* | *ΔW %* | *D ($gcm^{-3}$)* | *% of $D_{hp}$* | *α* | *β* | *AlN* | *$Sm_2O_3$* | *$Al_2O_3$* | *α'* | *β'* | *$SmAlO_3$* | *$M'_{SS}$* | *21R* |
|---|---|---|---|---|---|---|---|---|---|---|---|---|---|
| Green body | — | 2·067 | 61 | vs | w | m | m | — | — | — | — | — | — |
| 1200 | 0 | 2·212 | 65 | vs | w | m | — | — | — | — | m | — | — |
| 1300 | 0 | 2·238 | 66 | vs | w | m | — | — | — | — | m | — | — |
| 1400 | 0·1 | 2·303 | 68 | vs | w | m | — | — | — | — | m | vw | — |
| 1500 | 1·0 | 2·369 | 70 | s | w | w | — | — | vw | — | — | m | vw |
| 1600 | 1·3 | 2·445 | 72 | m | w | vw | — | — | m | w | — | m | vw |
| 1700 | 1·7 | 3·054 | 90 | w | w | — | — | — | s | mw | — | w | w |
| 1750 | 6·0 | 3·055 | 90 | — | — | — | — | — | vs | mw | — | vw | w |
| 1800 | — | 3·280 | 96 | — | — | — | — | — | vs | mw | — | — | w |
| 1850 | 5·9 | 3·325 | 98 | — | — | — | — | — | vs | mw | — | — | w |
| HP 1800 | 2·2 | 3·401 | 100 | — | — | — | — | — | vs | mw | — | | w |

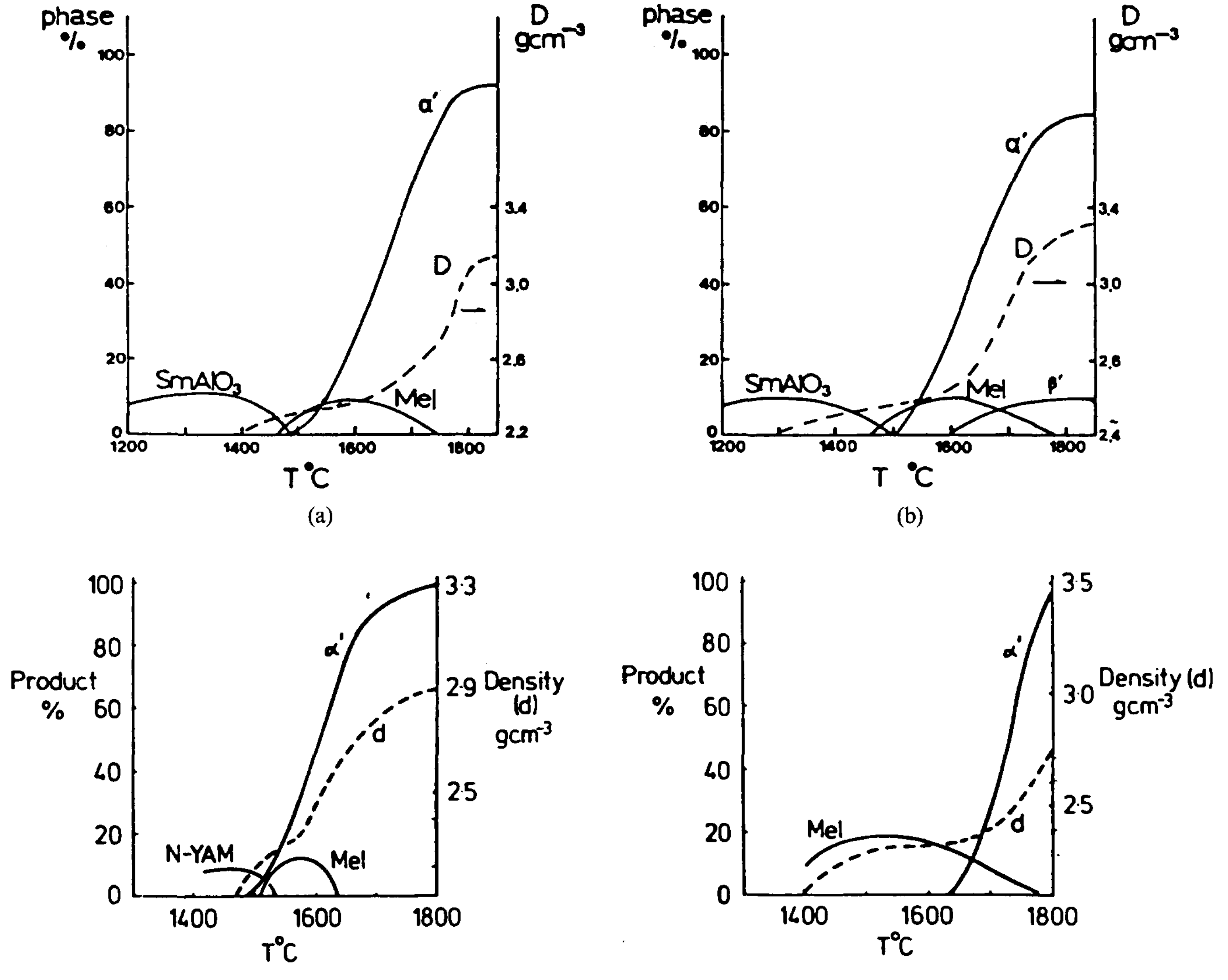

(a) (b)

(c) (d)

**Fig. 1.** Product phases and densification behaviour for samples (a) SA400 and (b) SA800 sintered for 1 h at different temperatures; also given are the data for (c) yttrium and (d) neodymium α' compositions sintered for 0·5 h at different temperatures.[4]

previously reported to be in equilibrium with $\alpha' + \beta'$ when yttria was used.[7] The closeness of phase boundaries in this part of the diagram is such that only a small compositional change is required to displace from one region to another, and phase proportions (particularly the $\alpha' : \beta'$ ratio) are extremely variable. These results indicate the existence of phase regions of the type α'–21R–27R–L (liquid) and α'–β'–21R–L at 1800°C in the Sm–Si–Al–O–N Jänecke prism.[5] Failure to identify 27R in sample SA400 may be due to strong overlaps between the 27R reflections and those of 21R and α' phases.

### 3.2 Densification of samarium α' ceramics

Figure 1 shows a summary of the results given in Tables 2 and 3, and also the related reaction sequences for yttrium and neodymium α-sialons.[2] The similarity between these systems is clearly shown. $M'_{SS}$ is an intermediate phase formed during sintering in all these systems and exhausts most of the liquid when it is precipitated, significantly retarding densification and the formation of α-sialons. As a result, a marked characteristic of these systems is that a rapid increase in densification does not occur until $M'_{SS}$ has finally melted. It is thought that the melting of $M'_{SS}$ yields a liquid that promotes densification and the formation of α' simultaneously. However, the final density of the samarium α' materials is much higher than comparable yttrium- and neodymium-densified samples (Table 4). More significantly, the Sm α' materials showed a higher rate of density increase during the rapid densifying stage compared with both the Y and Nd α' samples (Table 4), indicating that the samarium-containing liquid phase must possess a lower viscosity than the other two systems at the sintering temperature. The disappearance of Sm $M'_{SS}$ between 1750 and 1800°C suggests that the liquid-phase region in this system could be significantly displaced towards the nitrogen-rich side at the temperature range; whereas in the Nd system, the melilite phase persists even above 1850°C.[6] The closeness between the edge of

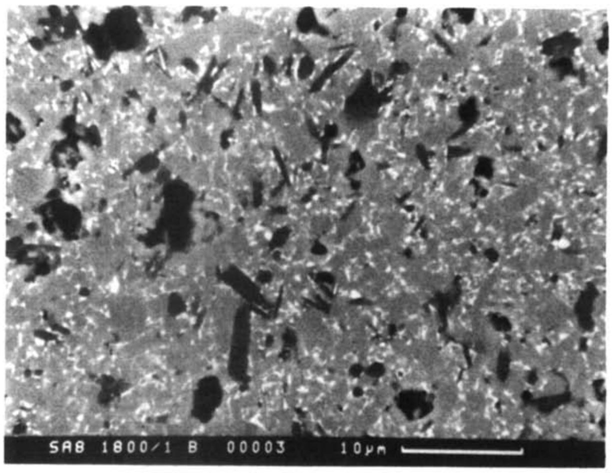
SAB 1800/1 B 00003 10μm

(a)

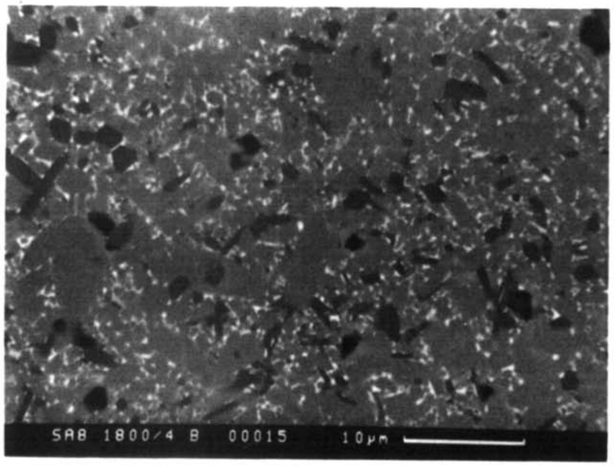
SAB 1800/4 B 00015 10μm

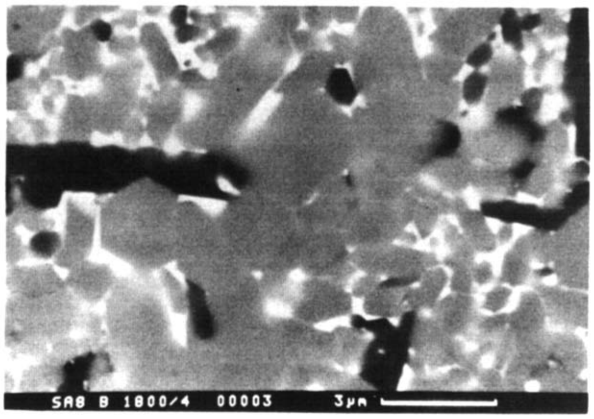
SAB B 1800/4 00003 3μm

**Table 6.** $Nd_2O_3$-containing α' compositions

| Sample | (mol %) | | | | (wt %) | | | |
|---|---|---|---|---|---|---|---|---|
| | $Si_3N_4$ | AlN | $Al_2O_3$ | $Nd_2O_3$ | $Si_3N_4$ | AlN | $Al_2O_3$ | $Nd_2O_3$ |
| NA4 | 48·22 | 46·58 | 1·96 | 3·24 | 67·89 | 19·16 | 2·01 | 10·94 |
| NA8 | 56·37 | 37·97 | 2·14 | 3·52 | 72·77 | 14·13 | 2·01 | 10·90 |

the possibility of further reducing the amount of grain boundary phase on a large scale by optimising the starting compositions; this is always claimed to be an advantage of α' materials.[8]

For comparison, two neodymium-containing compositions, equivalent to SA400 and SA800, were prepared, in which $Sm_2O_3$ was replaced by $Nd_2O_3$ in an equal mole percentage (Table 6). The samples were sintered at 1850°C for 2 h, in order to examine the effect of the 'melilite problem' reported in this system during densification.[2] The melilite phase observed in the Nd system is also an $M'_{SS}$[6] but did not completely dissolve in the liquid under the sintering conditions employed (Table 7). This is very different from the behaviour of Sm-containing samples, where no melilite phase was detected after sintering under either set of conditions used, i.e. 1800°C for 2 h or 1850°C for 1 h. The persistence of the $M'_{SS}$ phase reduces the amount of liquid available for densification and therefore the neodymium α' samples showed lower densities than the samarium ones. It is believed that the previous observations of the interruption of densification of β' and α' liquid compositions[2] was due to the persistence of the Nd $M'_{SS}$ phase at the sintering temperature employed. Therefore it is concluded that a moderate melting temperature of $M'_{SS}$ is a key issue when selecting a rare earth oxide for α' ceramics. Moreover, it is also noted that the yield of α' phase in the neodymium samples is lower compared to that in analogous samarium compositions, which may be because some neodymium cations are present as undissolved $M'_{SS}$ phase or because the neodymium α'-sialon region is smaller.

### 3.3 Heat-treatment of samarium α' ceramics

It would be desirable to produce a single-phase sialon material of the α' type. However, in practice, it is almost inevitable that some secondary glassy phase will remain. The softening of this grain boundary phase at about 1000–1200°C then severely degrades the high-temperature properties of these materials. Hence it is always desirable to devitrify residual glassy material into refractory crystalline phases in order to upgrade the high-temperature performance. For a sialon ceramic, there are two fundamental criteria governing the selection of intergranular phases, namely, that at the temperature at which the material is to be used, the grain boundary phase must neither react with the matrix nor soften or remelt, and also the product must possess good oxidation resistance. So far, YAG ($Y_3Al_5O_{12}$) has been widely accepted as the best intergranular phase for commercial β-sialon ceramics simply because it is one of a few viable alternatives; however, oxidation resistance of β'–YAG materials deteriorates rapidly above 1300°C.[9]

**Table 7.** Density and X-ray results for neodymium-containing samples sintered at 1850°C for 2 h

| Sample | D ($gcm^{-3}$) | α' (%)[a] | β' (%)[a] | 21R | $M'_{SS}$ |
|---|---|---|---|---|---|
| NA4 | 3·005 | vs (95) | vw (5) | w | w |
| NA8 | 3·294 | s (78) | m (22) | mw | w |

[a] Relative proportions between α' and β' phases.

Samples SA400 and SA800, previously sintered at 1800°C for 4 h, were heat-treated in nitrogen for 24 h between 1100 and 1600°C to study grain boundary devitrification. Table 8 shows X-ray results of the heat-treated materials. It is seen that $SmAlO_3$ readily forms in both samples when devitrified between 1200 and 1370°C and the phase may be stable to 1400°C as well if no β' is present in the sample. This is in contrast to the Nd–sialon system, in which neither β' nor α' is compatible with $NdAlO_3$.[2] A reduction in the z value for the β' phase after the formation of $SmAlO_3$ was observed and this may indicate a possible diffusion of Al from the β' structure into grain boundaries during heat-treatment. There was no β' phase in sample SA400 after heat-treatment, suggesting that more α' might also precipitate from the grain boundary glass to compensate for the crystallisation of $SmAlO_3$. A trace of melilite was found in sample SA800 at 1400°C. Above 1500°C, $SmAlO_3$ was completely remelted and melilite became the only intergranular phase. Simultaneously, some of the $Al_2O_3$ in the $SmAlO_3$ redissolved in the sialon phases and the amount of β' as well as its z value increased (Table 8). The melilite phase devitrified above 1500°C has been confirmed as being a form of aluminium-containing melilite solid solution ($M'_{SS}$) because of the remarkable increase in its cell dimensions compared to the original samarium melilite.[6]

Three samples, previously devitrified at 1370°C and 1500°C for 24 h respectively, were given an additional heat-treatment at 1100°C for 24 h but X-ray diffraction failed to find any new phase, although both samarium wollastonite and U-phase are stable at this temperature and the liquid composition is on the oxygen rich side of the α'–$SmAlO_3$ plane.[10] This implies that the amount of residual glass after the 1370°C and 1500°C de-

**Table 8.** X-Ray results of samples SA400 and SA800 after heat-treatment under different conditions

| | *(°C/h)* | *Crystalline phases* | | | | | *α'* | | *β'* | | |
|---|---|---|---|---|---|---|---|---|---|---|---|
| | | *α'(%)* | *β' (%)* | *21R* | *$SmAlO_3$* | *$M'_{SS}$* | *a(Å)* | *c(Å)* | *a(Å)* | *c(Å)* | *z* |
| SA400 | Before heat-treatment | vs | — | w | — | — | 7·816 | 5·698 | | | |
| | 1370/24 | vs | — | w | m | — | 7·817 | 5·695 | | | |
| | 1400/24 | vs | — | w | m | — | 7·817 | 5·699 | | | |
| SA800 | Before heat-treatment | vs(93) | w(7) | w | — | — | 7·841 | 5·692 | 7·622 | 2·921 | 0·61 |
| | 1200/24 | vs | w | w | mw | — | | | | | |
| | 1300/24 | vs(91) | mw(9) | w | mw | — | 7·810 | 5·690 | 7·617 | 2·921 | 0·53 |
| | 1370/24 | vs(89) | mw(11) | w | mw | — | 7·810 | 5·690 | 7·620 | 2·921 | 0·58 |
| | 1400/24 | vs(87) | mw(13) | w | mw | vvw | 7·811 | 5·691 | 7·620 | 2·921 | 0·58 |
| | 1500/24 | s(82) | m(18) | w | — | mw | 7·810 | 5·696 | 7·623 | 2·920 | 0·61 |
| | 1600/24 | s(75) | m(25) | w | — | mw | | | | | |
| | 1200/24 then 1600/24 | s(75) | m(25) | w | — | mw | | | | | |

vitrification treatments is quite small or that its composition has moved away from that of any crystalline phase stable at this temperature. On the other hand, the results may suggest that the liquid composition in the system has crossed the α'–$SmAlO_3$ plane at 1800°C, because both the two main devitrification products, $SmAlO_3$ and $M'_{SS}$, possess compositions either on the plane or on the nitrogen-rich side of the plane.

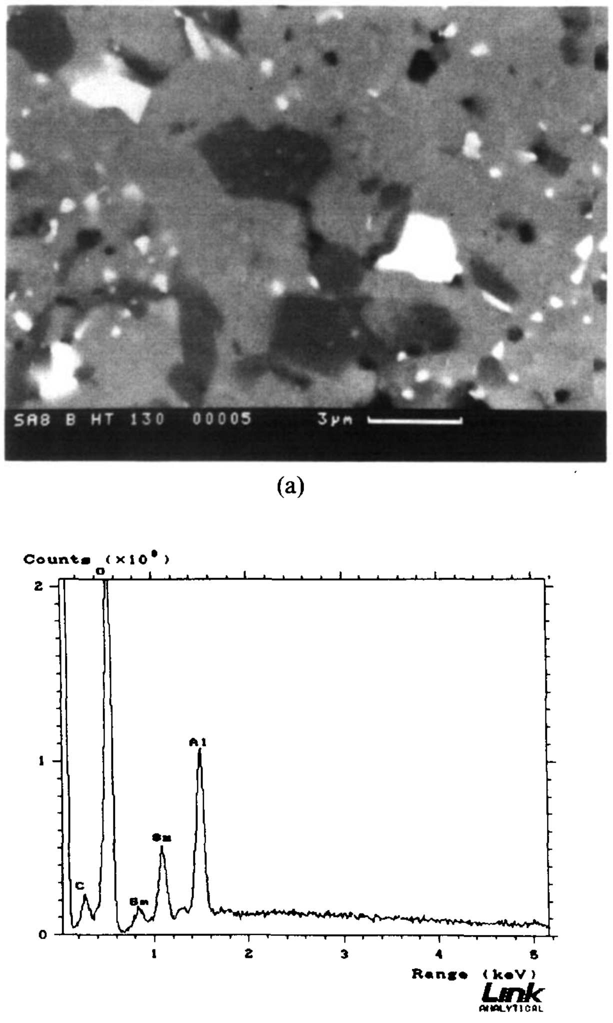

(a)

(b)

**Fig. 4.** (a) After heat-treatment at 1300°C for 24 h, the microstructure of sample SA800 consists of α' (light grey), β' (dark grey) and a crystalline grain boundary phase (white). (b) The EDAX result shows that the grain boundary phase is $SmAlO_3$. Pores in the boundary between $SmAlO_3$ and sialon grains are clearly visible. The surface of the sample was carbon coated.

### 3.4 Microstructures of α' ceramics after heat-treatment

Prior to heat-treatment, four phases, α'–β'–21R–glass, are in equilibrium in sample SA800. Figure 4 shows the microstructure of this sample after heat-treatment at 1300°C for 24 h. EDAX results confirm the phase transformation of grain boundary glass to $SmAlO_3$ after devitrification. Some large white grains of $SmAlO_3$ (about 3 μm) were found in the boundaries between sialon grains. Because there were no equivalent large areas of glassy phase in the sample before heat-treatment (Fig. 2), this must have formed by diffusion in the grain boundary during heat-treatment. The increase in submicron porosity in grain boundaries may be a result of this diffusion. It was also noticed that the widely distributed thin layer of intergranular phase between the sialon grains had been reduced, as a result of which, some large agglomerated sialon grains (particularly α') occur, separated by very little grain boundary phase.

Different microstructures were observed for sample SA800 after heat-treatment at 1500°C for 24 h (Fig. 5). At this temperature, the only grain boundary phase crystallised from the glass was $M'_{SS}$ ($Sm_2Si_2AlO_4N_3$), as clearly shown by its EDAX spectrum. An increase in the number of β' grains is also seen from these microstructures, suggesting that some α' → β' phase transformation has taken place during the heat-treatment. More significantly, the interface between the $M'_{SS}$ grains and the sialon matrix looks much clearer and denser compared with that between the $SmAlO_3$ and sialon grains. This kind of flawless grain boundary microstructure offers promise for improved mechanical properties at both ambient and elevated temperatures. The melting temperature of

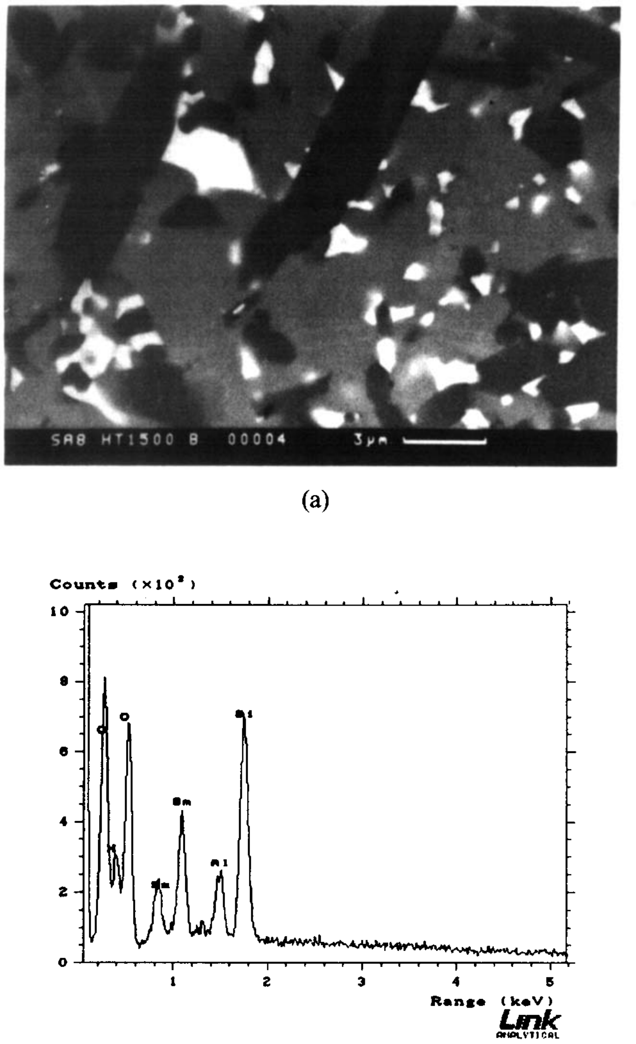

(a)

(b)

**Fig. 5.** (a) Microstructure of sample SA800 heat-treated at 1500°C for 24 h. (b) EDAX results confirm that the grain boundary phase (white) is $M'_{SS}$ ($Sm_2Si_2AlO_4N_3$). Notice the intimate contact at the interfaces between $M'_{SS}$ and sialon grains compared with the microstructure shown in Fig. 4. The surface of the sample was carbon coated.

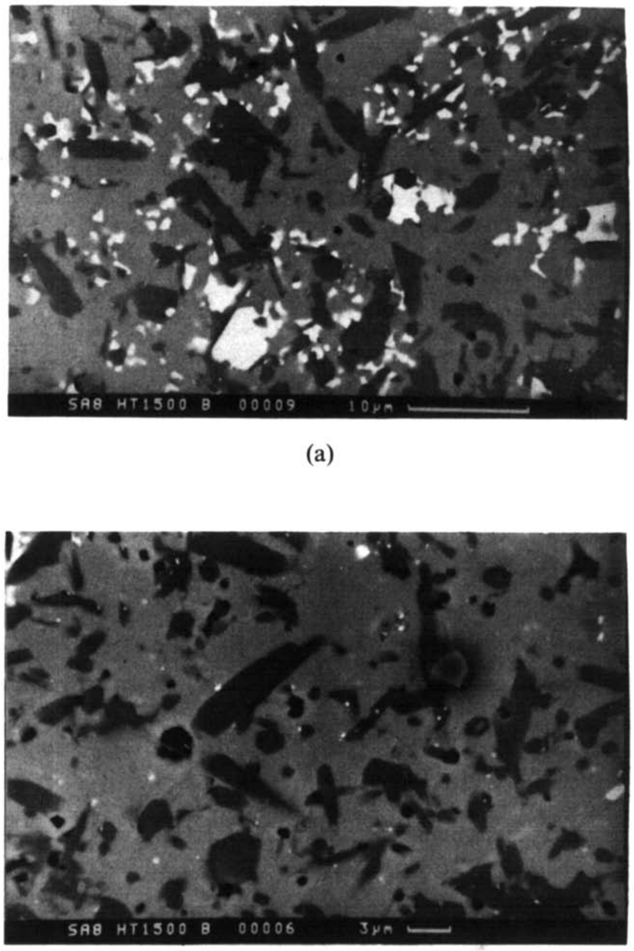

(a)

(b)

**Fig. 6.** Different microstructures of the same sample (SA800) heat-treated at 1500°C for 24 h. It is seen that areas with relatively large amounts of grain boundary phase (white) (a) are much denser than those with less grain boundary phase (b). Pores are always associated with areas having little grain boundary phase. The dark grey phases are mainly $\beta'$ with a small amount of 21R. Comparing these microstructures with that in Fig. 2 (prior to heat-treatment), phase transformation from $\alpha' \rightarrow \beta'$ during heat-treatment is clearly apparent.

the Sm oxynitride glass is about 1350°C[11] and therefore the crystallisation of grain boundary glass taking place below 1350°C corresponds to a conventional glass–ceramic process. When samples are heat-treated above the melting temperature of the grain boundary glass, the fusion of the grain boundary forms a liquid which can induce chemical reactions with the sialon matrix and allows particle rearrangement as well as precipitation of new phase(s). In other words, the crystallisation of the grain boundary phase above the glass melting temperature suggests a fusion and precipitation process. The intimate interfaces between the $M'_{SS}$ and sialon grains are the result of this fusion and precipitation process. However, an increase in porosity in some areas of the same sample is also observed after devitrification at 1500°C (Fig. 6). It is very interesting to find that the porosity increase always occurs in areas where the grain boundary phase has almost entirely disappeared. Although areas with limited amounts of grain boundary glass were observed in the as-fired samples, this kind of extreme inhomogeneity in the grain boundary microstructure was clearly not a feature of the materials prior to heat-treatment. It seems that grain boundary diffusion from one area to the other has taken place during this high-temperature heat-treatment and this remains a topic for further investigations.

## 4 Conclusions

Sm $\alpha'$ ceramics show superior densification behaviour compared with equivalent compositions in the Nd system. As a result, materials with 99% of the density of the hot-pressed $\alpha'$ sample have been formed by pressureless sintering at 1800°C for 4 h. The relatively low melting temperature of the Sm

M'$_{SS}$ phase formed during sintering is mainly responsible for the improved performance in densification. The introduction of a small amount of $\beta'$ phase (about 10%) into $\alpha'$ materials significantly improves the densification behaviour. Two grain boundary phases have been formed during post-sintering heat-treatment at different temperatures. Below 1400°C, $SmAlO_3$ is stable, but between 1400 and 1600°C, the Al-containing melilite solid solution (M'$_{SS}$) is the only crystalline phase in the grain boundaries. Different microstructures can be produced by heat-treatment at different temperatures. Low-temperature heat-treatment produces some pores in the grain boundaries whereas at higher temperatures the enhanced grain boundary diffusion creates a flawless microstructure between M'$_{SS}$ and sialon grains, although some inhomogeneities are observed in other areas.

## Acknowledgment

The financial support by Cookson Group plc UK during the period when the work was carried out is sincerely appreciated.

## References

1. Ekström, T. & Nygren, M., Sialon ceramics. *J. Am. Ceram. Soc.*, **75** (1992) 259–76.
2. Slasor, S., Liddell, K. & Thompson, D. P., The role of $Nd_2O_3$ as an additive in the formation of $\alpha'$ and $\beta'$ sialons. In *Special Ceramics 8*, ed. S. P. Howlett & D. Taylor. The Institute of Ceramics, 1986, pp. 51–64.
3. Mitomo, M., In situ microstructure control in silicon nitride based ceramics. In *Advanced Ceramics II*, ed. S. Somiya. Elsevier, UK, 1988, pp. 147–61.
4. Ekström, T., Effect of composition, phase content and microstructure on the performance of yttrium sialon ceramics. *Mater. Sci. Eng.*, **A109** (1989) 341–9.
5. Cheng, Y.-B. & Thompson, D. P., Pressureless sintering of samarium-containing $\alpha'$-sialon ceramics (in press).
6. Cheng, Y.-B. & Thompson, D. P., Aluminium-containing nitrogen melilite phases. *J. Am. Ceram. Soc.* **77** (1994) 143–8.
7. Slasor, S. & Thompson, D. P., *J. Mater. Sci. Lett.*, **6** (1987) 315–16.
8. Jack, K. H., In *Ceramics and Civilisation*, Vol. 3, The American Ceramic Society, 1987, pp. 259–88.
9. Lewis, M. H., Mason, S. & Szweda, A., Sialon ceramic for application at high temperature and stress. In *Non-Oxide Technical and Engineering Ceramics*, ed. S. Hampshire. Elsevier Applied Science, London, 1986, pp. 175–90.
10. Mandal, H., Thompson, D. P. & Ekström, T., Heat treatment of sialon ceramics densified with higher atomic number rare earth and mixed yttrium/rare earth oxides. In *Special Ceramics 9*, ed. R. Stevens. The Institute of Ceramics, 1992, pp. 97–104.
11. Cheng, Y.-B. & Thompson, D. P., Unpublished Internal Report (III) to Cookson Group plc, April 1990.